Int. J. Adv. Appl. Math. and Mech. 4(1) (2016) 1 – 10 (ISSN: 2347-2529)
Journal homepage: www.ijaamm.com

International Journal of Advances in Applied Mathematics and Mechanics

Analytical study of MHD boundary layer flow and heat transfer towards a porous exponentially stretching sheet in presence of thermal radiation

Research Article

Kalpna Sharma[a], **Sumit Gupta**[b,*]

[1] *Department of Mathematics, Manipal University Jaipur, Dehmi Kalan, Jaipur-Ajmer Expressway, Jaipur-303007, Rajasthan, India*
[b] *Department of Mathematics, Swami Keshvanand Institute of Technology, Management and Gramothan, Ramnagaria, Jaipur -302017, Rajasthan, India*

Received 04 May 2016; accepted (in revised version) o5 August 2016

Abstract: In this present article, we have analyzed MHD boundary layer flow of a viscous incompressible fluid over an exponentially porous stretching sheet in presence of thermal radiation. Using a similarity transformation, the governing equations are transformed into a system of nonlinear ordinary differential equations, which are then solved by homotopy analysis method (HAM). The effects of various parameters, namely the magnetic field parameter, radiation parameter, suction parameter, permeability parameter, Prandtl number on the velocity and temperature are analyzed through graphically. Moreover, a comparative study between the previously published and the present study is made.

MSC: 76S05 • 76M55

Keywords: MHD boundary layer flow • Similarity transformation • HAM • Prandtl number

1. Introduction

The flow over a stretching sheet has been premeditated because of its numerous industrial applications such as industrialized of polymer sheet, filaments and wires, through the mechanized process. The stirring sheet is assumed to extend on its own plane and the protracted surface interacts with ambient fluid both impulsively and thermally. Sakiadas [1] was the first who discuss the boundary layer flow over a surface. He discussed numerical solutions of laminar boundary-layer behavior on a moving continuous flat surface. Experimental and analytical behavior of this problem was presented by Tsou et al. [2] to show that such a flow is physically by validating Sakiadas [1] work. Crane [3] extended the work of Sakiadas [1] for both linearly and exponentially stretching sheet considering steady two-dimensional viscous flow. Free convective on a vertical stretching surface was discussed by Wang [4]. Heat transfer analysis over an exponentially stretching continuous surface with suction was presented by Elbashbeshy [5]. He obtained similarity solutions of the laminar boundary layer equations describing heat and flow in a quiescent fluid driven by an exponentially stretching surface with suction. Viscoelastic MHD flow heat and mass transfer over a stretching sheet with dissipation of energy and stress work was discussed by Khan et al. [6]. Ishak et al. [7] studied heat transfer over a stretching surface with variable heat flux in micropolar fluids. Nadeem et al. [8] coated boundary layer flow of a Jeffrey fluid over an exponential stretching surface with radiation effects. Recently Nadeem et al. [9] investigated the MHD boundary layer flow of a Casson fluid over an exponentially permeable stretching sheet. Many researchers such as Gupta and Gupta [10] , Datta et al. [11] and Chen and Char [12] extended the work of Crane [3] by including the effect of heat and mass transfer analysis under different physical situations. On the other hand, Gupta and Gupta [13] stressed that realistically, stretching surface is not necessarily continuous. Most of the available literature deals with the study of boundary layer flow over a stretching surface where the velocity of the stretching surface is assumed linearly proportional to the distance from the fixed origin. However, it is often argued that [13] realistically stretching of plastic sheet may not necessarily be linear. This situation was beautifully dealt by Kumaran and Ramanaiah [14] in their work on boundary layer fluid flow where, probably first time, a general quadratic stretching sheet has been assumed. Recently, various aspects of such problem have

* Corresponding author.
E-mail address: guptasumit.edu@gmail.com (Sumit Gupta).

Nomenclature

M	Magnetic parameter
Pr	Prandtl number
S	Suction/Injection parameter
St	Stratification parameter
T	Temperature of the fluid
$T_w(x)$	Prescribed surface temperature
$T_\infty(x)$	Variable free-stream temperature
u, v	Component of velocity in $x-$ and $y-$ directions
R_d	Radiation parameter
k_1	Permeability parameter
k^*	Absorption coefficient
Nu	Local Nusselt number
Greek symbols	
η	Similarity variable
κ	The coefficient of thermal conductivity
μ	Dynamic viscosity
σ	Stefan-Boltzman constant
ν	Kinematic viscosity
ψ	Stream function
ρ	Density of the fluid
θ	Non-dimensionless temperature

been investigated by many authors such as Xu and Liao [15] , Cortell [16, 17] , Hayat et al. [18] , and Hayat and Sajid [19]. Mandal and Mukhopadhyay [20, 21] studied the heat transfer analysis over an exponentially stretching sheet through porous and stratified medium.

Suction or injection (blowing) of a fluid through the bounding surface can significantly change the flow field. In general, suction tends to increase the skin friction whereas injection acts in the opposite manner. Injection or withdrawal of fluid through a porous bounding wall is of general interest in practical problems involving boundary layer control applications such as film cooling, polymer fiber coating, coating of wires, etc. The process of suction and blowing has also its importance in many engineering activities such as in the design of thrust bearing and radial diffusers, and thermal oil recovery. Suction is applied to chemical processes to remove reactants. Blowing is used to add reactants, cool the surface, prevent corrosion or scaling and reduce the drag.

One of the important aspects in this study is the investigation of heat transfer processes. This is due to the fact that the rate of cooling influences a lot to the quality of the product with desired characteristics. Continuous surface heat transfer problems have many practical applications in industrial manufacturing processes. Such processes are hot rolling, wire drawing and glass fiber production. Problems with variable surface heat flux have been introduced in many other studies [22, 23]. In modeling the boundary layer flow and heat transfer of these problems, the boundary conditions that are usually applied are either a specified surface temperature or a specified surface heat flux.

Homotopy analysis method (HAM), proposed by Liao [24–26], is a very powerful method and has been employed by numerous researchers in various physical phenomena [27–32]. Recent works on the Newtonian and non-Newtonian fluids with different geometries can be found in [33–38]. The purpose of this present work is to extend the flow and heat transfer analysis in boundary layer over an exponentially stretching sheet with radiation embedded in a stratified medium. Using suitable transformations, a third order ordinary differential equation corresponding to the momentum equation and a second order differential equation corresponding to the heat equation are derived.

2. Mathematical formulations

Let us consider the flow of an incompressible viscous fluid past a flat sheet coinciding with the plane $y = 0$ in a porous medium with a non-uniform permeability k. In this analysis of the flow in the porous medium, the differential equation governing the fluid motion is based on DarcyâĂŹs law, which accounts for the drag exerted by the porous medium [39, 40]. In a fluid flow through porous medium, the pressure drop caused by the frictional drag is directly proportional to the velocity for low speed flow. This is the familiar Darcy's law. At higher velocities, inertial effects become appreciable, causing an increase in the form drag [41]. Here the effects of a solid boundary and the inertial effects have been neglected. These effects become more significant near the boundary and in a media with high porosity [42, 43]. It is assumed that the sheet is

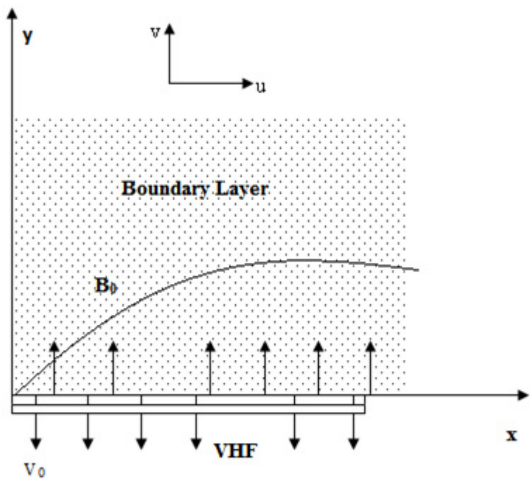

Fig. 1. Schamatic diagram of the problem.

subjected to a variable heat flux (VHF) $q_w(x)$.The fluid flow is confined to $y > 0$. Two equal and opposite forces are applied along the x-axis so that the wall is stretched keeping the origin fixed. The effect of these two equal and opposite forces cause a symmetric boundary at the center (the origin as shown in Fig. 1) of the porous medium. A variable magnetic field $B(x) = B_0 e^{\frac{x}{2L}}$ is applied normal to the sheet, B_0 being a constant. The sheet of temperature $T_w(x)$ and is embedded in a thermally stratified medium of variable ambient temperature $T_\infty(x)$ where $T_w(x) > T_\infty(x)$. It is assumed that $T_w(x) = T_0 + c\,e^{\frac{x}{2L}}$ where T_0 is the reference temperature, $b > 0$, $c \geqslant 0$ are constants.

The continuity, momentum and energy equations governing such type of flow are written as

$$\frac{\partial u}{\partial x}+\frac{\partial v}{\partial y}=0, \tag{1}$$

$$u\frac{\partial u}{\partial x}+v\frac{\partial u}{\partial y}=\frac{\partial^2 u}{\partial y^2}-\frac{v}{k}u-\frac{\sigma B^2}{\rho}u, \tag{2}$$

$$u\frac{\partial T}{\partial x}+v\frac{\partial T}{\partial y}=\frac{\kappa}{\rho c_p}\frac{\partial^2 T}{\partial y^2}-\frac{1}{\rho c_p}\frac{\partial q_r}{\partial y}, \tag{3}$$

with the following boundary conditions

$$\left.\begin{array}{ll} u=U, & v=-V(x), \\ T=T_w(x), & \dfrac{\partial T}{\partial y}=-\dfrac{q_w(x)}{\kappa}\end{array}\right\} \quad \text{at} \quad y=0; \tag{4}$$

$$u\to 0, \quad T\to T_\infty \quad \text{as} \quad y\to\infty. \tag{5}$$

where and are the components of velocity respectively in the x and y directions, $\upsilon=\frac{\mu}{\rho}$ is the kinematics viscosity, ρ is fluid density, μ is the coefficient of fluid viscosity, c_p is specific heat at constant pressure and κ is the thermal conductivity of the fluid. $U=U_0 e^{\frac{x}{L}}$ is the stretching velocity, U_0 is reference velocity, $V(x)>0$ is velocity of suction and $V(x)<0$ is velocity of blowing, $V(x)=V_0\, e^{\frac{x}{2L}}$, a special type of velocity at the wall is considered. V_0 is the initial strength of suction.

Following Rosseland approximation [1972] the radiative heat flux q is modeled as

$$q_r=-\frac{4\sigma}{3k^*}\frac{\partial T^4}{\partial y} \tag{6}$$

where σ is the Stefan-Boltzman constant, and k^* is the absorption coefficient.

Assuming that the differences in the temperature within the flow are such that T^4 can be expressed as a linear combination of the temperature, one can expand T^4 in a Taylor's series about T_∞ as follows.

$$T^4=T_\infty^4+4T_\infty^3(T-T_\infty)+6T_\infty^2(T-T_\infty)^2+\dots \tag{7}$$

By neglecting the higher order terms beyond the first degree in $(T-T_\infty)$, we get

$$T^4=4T_\infty^3 T-3T_\infty^4, \tag{8}$$

Substituting in (6), we get

$$q_r=-\frac{16\sigma T_\infty^3}{3k^*}\frac{\partial T}{\partial y}. \tag{9}$$

On differentiation we get

$$\frac{\partial q_r}{\partial y}=-\frac{16\sigma T_\infty^3}{3k^*}\frac{\partial^2 T}{\partial y^2}. \tag{10}$$

The following relation are now introduced for u, v and $\theta(\eta)$ as

$$u=\frac{\partial\psi}{\partial y},\quad v=-\frac{\partial\psi}{\partial x},\quad \theta(\eta)=\frac{T-T_\infty}{T_w-T_\infty}$$

where $\psi(x,y)$is the stream function.

Using the similarity transformation

$$\left.\begin{array}{l} \eta=\sqrt{\dfrac{U_0}{2\upsilon L}}e^{\frac{Nx}{2L}}y, \\ u=U_0 e^{\frac{Nx}{L}}f'(\eta),\ v=-N\sqrt{\dfrac{\upsilon U_0}{2\upsilon L}}e^{\frac{Nx}{L}}\{f(\eta)+\eta f'(\eta)\}, \\ T=\dfrac{q_{w0}}{\kappa}T_0 e^{\frac{Nx}{L}}\theta(\eta), \end{array}\right\} \tag{11}$$

Now substituting Eqs.(6)-(11) in Eq.(2) and (3), the governing equations transform to

$$f'''+Nff''-2Nf'^2-(k_1+M)f'=0, \tag{12}$$

$$\left(1+\frac{4}{3}R_d\right)\theta''+\Pr(f\theta'-\theta f')-\Pr Stf'=0. \tag{13}$$

with the following boundary conditions

$$f'=1,\quad f=S,\quad \theta=1-St \quad \text{at} \quad \eta=0; \tag{14}$$

$$f'\to 0,\quad \theta\to 0 \quad \text{as} \quad \eta\to\infty. \tag{15}$$

Where the prime denotes differentiation with respect to η , $M=\frac{2\sigma {B_0}^2 L}{\rho U_0}$ is the magnetic parameter, $S=\frac{v_0}{\sqrt{\frac{U_0 v}{2L}}}>0\,(\text{or}<0)$ is the suction (blowing) parameter, $St=\frac{c}{b}$ is the stratification parameter and $\Pr=\frac{\mu c_p}{\kappa}$ is the Prandtl number, $R_d=\frac{16T_\infty^3\sigma}{3kk^*}$ is the radiative parameter , N is the exponentially stretching sheet parameter, $k_1=\frac{2\upsilon L}{k_0 U_0}$ is the permeability parameter, $St>0$ implies a stably stratified environment, while $St=0$ corresponds to an unstratified environment.

The physical quantities of interest in this problem as reported by Lai and Kulacki [44] are the skin friction coefficient and the Nusselt number which are defined as

Skin friction coefficient:

$$C_f=-\frac{U_0}{x\sqrt{2}}\left(\frac{\partial u}{\partial y}\right)_{y=0}=f''(0) \tag{16}$$

Nusselt number:

$$Nu=\frac{xq_w}{k(T_w-T_\infty)}=-\theta'(0) \tag{17}$$

3. Homotopy analysis solutions

We express $f(\eta)$ and $\theta(\eta)$ by a set of base functions [45]

$$f(\eta)=a_{0,0}^0+\sum_{n=0}^{\infty}\sum_{k=0}^{\infty}a_{m,n}^k\eta^k\exp(-n\eta), \tag{18}$$

$$\theta(\eta)=\sum_{n=0}^{\infty}\sum_{k=0}^{\infty}b_{m,n}^k\eta^k\exp(-n\eta). \tag{19}$$

In which $a_{m,n}^k$ and $b_{m,n}^k$ are the coefficients. By rule of solution expressions and the boundary conditions (14)-(15), the initial guesses f_0 and θ_0 are selected as

$$f_0(\eta)=1+S+\exp(-\eta), \tag{20}$$

$$\theta_0(\eta)=(1-St)\exp(-\eta). \tag{21}$$

With the linear operators as

$$L_f=\frac{d^3 f}{d\eta^3}-\frac{df}{d\eta}, \tag{22}$$

$$L_\theta = \frac{d^2\theta}{d\eta^2} - \theta, \tag{23}$$

With the property that

$$L_f\left[C_1 + C_2\exp(-\eta) + C_3\exp(\eta)\right] = 0, \tag{24}$$
$$L_\theta\left[C_4\exp(-\eta) + C_5\exp(\eta)\right] = 0. \tag{25}$$

Where $C_i,\ i = 1..5$ are arbitrary constants.

The zeroth order deformation problems can be written as

$$(1-p)L_f[\hat{f}(\eta;p) - f_0(\eta)] = p\hbar_f N_f[\hat{f}(\eta;p)], \tag{26}$$

$$(1-p)L_\theta[\hat{\theta}(\eta;p) - \theta_0(\eta)] = p\hbar_\theta N_\theta[\hat{f}(\eta;p),\hat{\theta}(\eta;p)]. \tag{27}$$

With the boundary conditions

$$\left.\begin{array}{l} f'(0;p) = 1,\quad f(0;p) = S,\quad \theta(0;p) = 1 - St \\ f'(\infty;p) = 0,\quad \theta(\infty;p) = 0 \end{array}\right\} \tag{28}$$

Where $p \in [0,1]$ indicates the embedding parameter and $\hbar_f$ and $\hbar_\theta$ the nonzero auxiliary parameters. Moreover the nonlinear operators N_f and N_θ are prescribed as

$$N_f[\hat{f}(\eta;p)] = \frac{\partial^3\hat{f}(\eta;p)}{\partial\eta^3} + N\hat{f}(\eta;p)\frac{\partial^2\hat{f}(\eta;p)}{\partial\eta^2} - 2N\left(\frac{\partial\hat{f}(\eta;p)}{\partial\eta}\right)^2 - (k_1+M)\frac{\partial\hat{f}(\eta;p)}{\partial\eta}, \tag{29}$$

$$N_\theta[\hat{f}(\eta;p),\hat{\theta}(\eta;p)] = \left(1+\frac{4}{3}R_d\right)\frac{\partial^2\hat{\theta}(\eta;p)}{\partial\eta^2} + \Pr\left(N\frac{\partial\hat{\theta}(\eta;p)}{\partial\eta}\hat{f}(\eta;p) - N\frac{\partial\hat{f}(\eta;p)}{\partial\eta}\hat{\theta}(\eta;p)\right) - \Pr St\frac{\partial\hat{f}(\eta;p)}{\partial\eta}. \tag{30}$$

For $p = 0$ and $p = 1$ we have

$$\hat{f}(\eta;0) = f_0(\eta),\quad \hat{f}(\eta;1) = f(\eta), \tag{31}$$
$$\hat{\theta}(\eta;0) = \theta_0(\eta),\quad \hat{\theta}(\eta;1) = \theta(\eta). \tag{32}$$

By means of Taylor's series we have

$$\hat{f}(\eta;p) = f_0(\eta) + \sum_{m=1}^{\infty} f_m(\eta)p^m, \tag{33}$$

$$\hat{\theta}(\eta;p) = \theta_0(\eta) + \sum_{m=1}^{\infty} \theta_m(\eta)p^m. \tag{34}$$

$$\left.\begin{array}{l} f_m(\eta) = \dfrac{1}{m!}\left(\dfrac{\partial^m f(\eta;p)}{\partial\eta^m}\right)_{p=0}, \\ \theta_m(\eta) = \dfrac{1}{m!}\left(\dfrac{\partial^m\theta(\eta;p)}{\partial\eta^m}\right)_{p=0}. \end{array}\right\} \tag{35}$$

The auxiliary parameters are so properly chosen that series (33)-(34) converges when $p = 1$ and thus

$$f(\eta) = f_0(\eta) + \sum_{m=1}^{\infty} f_m(\eta), \tag{36}$$

$$\theta(\eta) = \theta_0(\eta) + \sum_{m=1}^{\infty} \theta_m(\eta). \tag{37}$$

The resulting problems at the mth-order deformation are

$$L_f[f_m(\eta) - \chi_m f_{m-1}(\eta)] = \hbar_f\Re_m^f(\eta), \tag{38}$$
$$L_\theta[\theta_m(\eta) - \chi_m\theta_{m-1}(\eta)] = \hbar_\theta\Re_m^\theta(\eta), \tag{39}$$
$$f'_m(0) = 0,\ f_m(0) = 0,\ \theta_m(0) = 0. \tag{40}$$
$$f'_m(\infty) = 0,\ \theta_m(\infty) = 0 \tag{41}$$

With the following definitions

$$\Re_m^f(\eta) = f'''_{m-1} + N\sum_{k=0}^{m-1} f_k f''_{m-1-k} - 2N\sum_{k=0}^{m-1} f'_k f'_{m-1-k} - (k_1+M)f'_{m-1}, \tag{42}$$

$$\Re_m^\theta(\eta) = \left(1+\frac{4}{3}R_d\right)\theta''_{m-1} + N\Pr\sum_{k=0}^{m-1}\left(f_k\theta'_{m-1-k} - f'_k\theta_{m-1-k}\right) - \Pr St f'_{m-1}. \tag{43}$$

In which

$$\chi_m = \begin{cases} 0, & m \leqslant 1, \\ 1, & m > 1, \end{cases} \tag{44}$$

The general solutions of Eqs. (38)-(39) can be written as

$$f_m(\eta) = f_m^*(\eta) + C_1 + C_2\exp(-\eta) + C_3\exp(\eta), \tag{45}$$
$$\theta_m(\eta) = \theta_m^*(\eta) + C_4\exp(-\eta) + C_5\exp(\eta). \tag{46}$$

In which $f_m^*(\eta)$ and $\theta_m^*(\eta)$ are the particular solutions of the Eqs. (42)-(43). Note that the (42)-(43) can be solved by Mathematica, Maple and Matlab one after the other in the order $m = 1,2,3,\ldots$

3.1. Convergence of the homotopy solutions

It can be noticed that the series solutions (45)-(46) contain the non-zero auxiliary parameters $\hbar_f$ and $\hbar_\theta$. We can adjust and control the convergence of the HAM solutions with the help of these auxiliary parameters. Hence to compute the range of admissible values of $\hbar_f$ and $\hbar_\theta$, we display the $\hbar$ -curve of the functions $f''(0)$ and $\theta'(0)$ of 15th-order of approximations. Fig. 2 depicts that the range of admissible values of $\hbar_f$ and $\hbar_\theta$ are $-1.8 \leqslant \hbar_f \leqslant -0.15$ and $-1.8 \leqslant \hbar_\theta \leqslant -0.2$. The series solution (45)-(46) converge in the whole region of η when $\hbar_f = \hbar_\theta = -1.2$.

Table 1 indicates that 15^{th} order approximation gives a convergent series solution HAM solutions of for several values of Prandtl number Pr. Also in Table 2, numerical values of skin friction coefficients for different parameters are determined.

4. Results and discussion

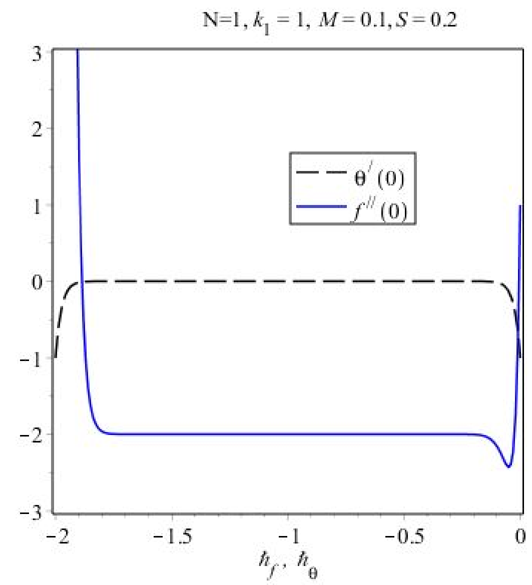

Fig. 2. $\hbar_f$ and $\hbar_\theta$ curve for functions f and θ for 15^{th}-order of HAM approximations.

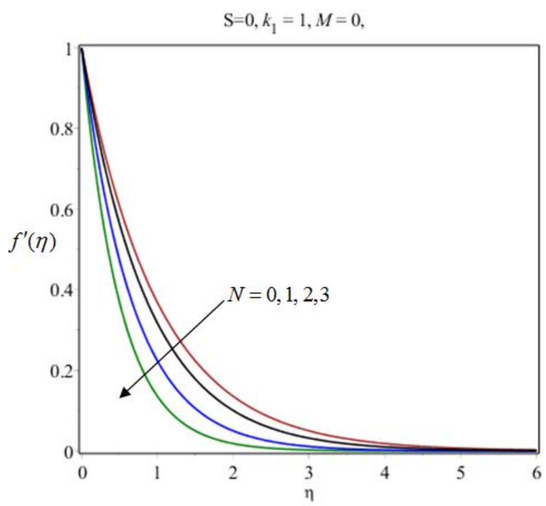

Fig. 3. Variation of velocity $f'(\eta)$ with η for several values of exponential parameter N in absence of suction.

The main objective here is to study the variations of emerging physical parameters on the fluid flow and heat transfer. In order to provide a physical insight into the flow problem, Figs. 3-19 are plotted for the velocity, temperature and heat transfer. Fig. 3 depicts the dimensionless veloc-

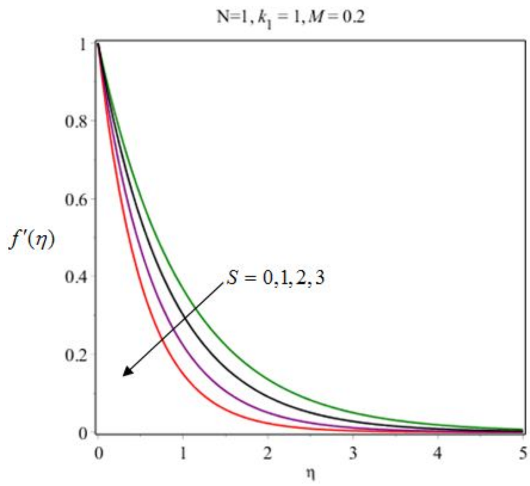

Fig. 4. Variation of velocity $f'(\eta)$ with η for several values of suction/blowing parameter *S*.

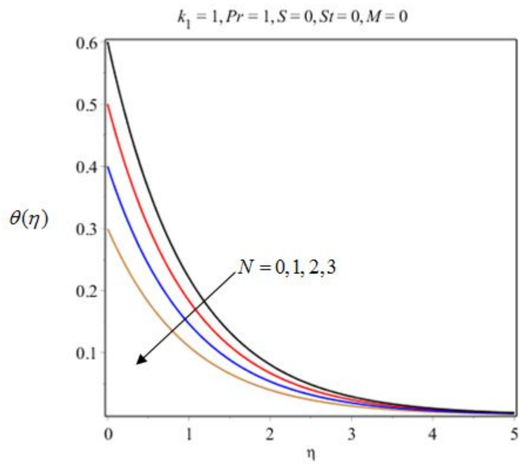

Fig. 5. Variation of temperature $\theta(\eta)$ with η for several values of exponential parameter N in absence of suction.

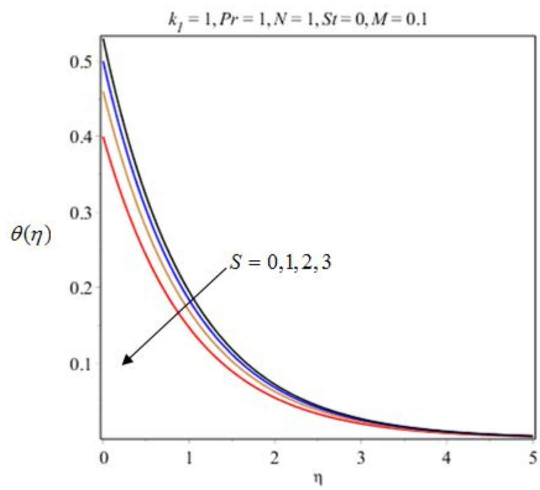

Fig. 6. Variation of temperature $\theta(\eta)$ with η for several values of suction/blowing parameter *S*.

Table 1. Comparison of HAM solutions of $-\theta'(0)$ for several values of Prandtl number.

Pr	Magyari and Keller [13]	Bidin and Nazar [22]	El-Aziz [23]	Ishak [7]	Mandal and Mukhopadhyay [21]	Present
1	0.9548	0.9547	0.9548	0.9548	0.9547	0.9547
2		1.4714		1.4715	1.4714	1.4714
3	1.8691	1.8691	1.8691	1.8691	1.8691	1.8691
5	2.5001		2.5001	2.5001	2.5001	2.5001
10	3.6604		3.6604	3.6604	3.6604	3.6604

Table 2. Numerical Values of skin friction coefficient $f''(0)$ for various parameters.

M	S	k_1	N	$f''(0)$
0.2	0.1	0.1	1	-1.17301
0.4				-1.25142
0.6				-1.28180
0.2	0.1			-1.17212
	0.5			-1.12475
	0.7			-1.07563
	0.1	0.1		-1.14566
		0.3		-1.23459
		0.5		-1.35664
		0.1	1	-1.25823
			1.3	-1.34560
			1.5	-1.28933

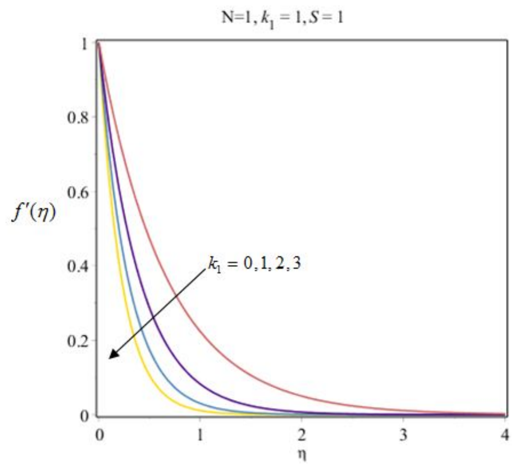

Fig. 8. Variation of velocity $f'(\eta)$ with η for several values of permeability parameter k_1 in presence of suction.

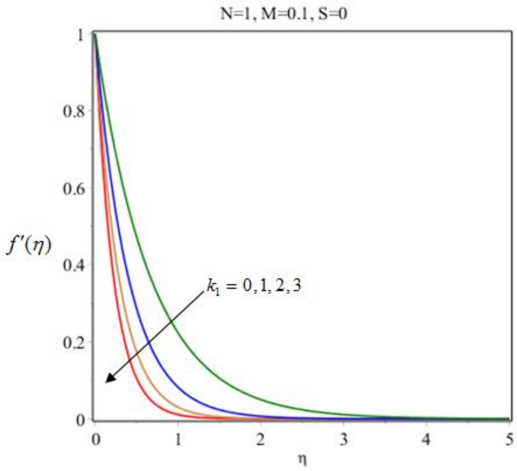

Fig. 7. Variation of velocity $f'(\eta)$ with η for several values of permeability parameter k_1 in absence of suction.

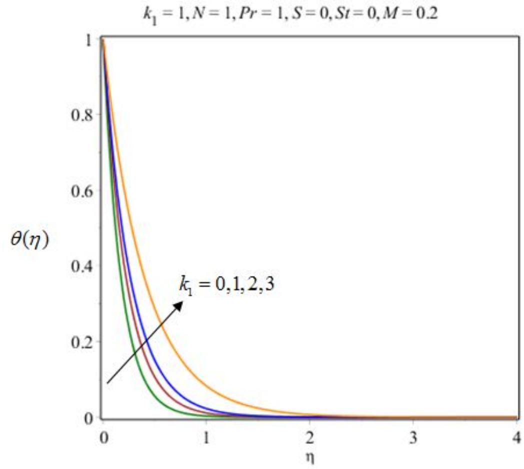

Fig. 9. Variation of temperature $\theta(\eta)$ with η for several values of permeability parameter k_1 in absence of suction.

ity profiles of $f'(\eta)$ for several values of exponential parameter N. while Fig. 4 depicts the dimensionless velocity profiles of $f'(\eta)$ for several values of suction/injection parameter S. velocity is decreasing for both suction/injection parameter and exponential parameter N. In Fig. 4, the velocity decreases significantly with increasing suction whereas fluid velocity is found to be increase with blowing. It is observed that, when the wall suction ($S > 0$) is considered, this causes a decrease in the boundary layer thickness and the velocity field is reduced. $S = 0$ represents the case of non-porous stretching sheet. Opposite behavior is noted for blowing ($S < 0$) parameter. The physical explanation for such a behavior is that while stronger blowing is provided, the heated fluid is pushed farther from the wall where due to less influence of the viscosity, the flow is accelerated. This effect acts to increase maximum velocity within the boundary layer. Figs. 5-6 depicts the effect of exponential parameter N and suction/ injection parameters on temperature. From Fig. 5, it is noted that the wall temperature decrease throughout in the boundary layer for positive values of exponential parameter N. Fig. 6 represents the temperature profiles for variable suction/ injection parameter S with variable heat flux.

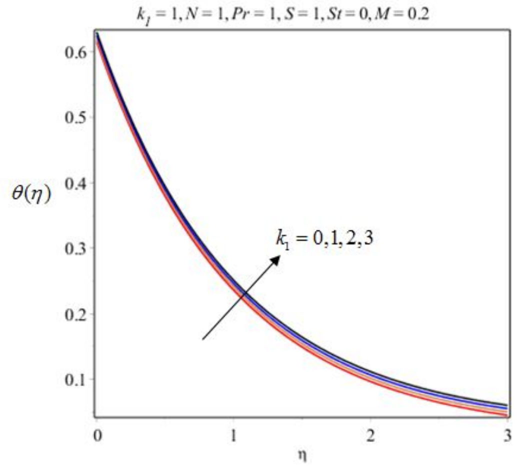

Fig. 10. Variation of temperature $\theta(\eta)$ with η for several values of permeability parameter k_1 in presence of suction.

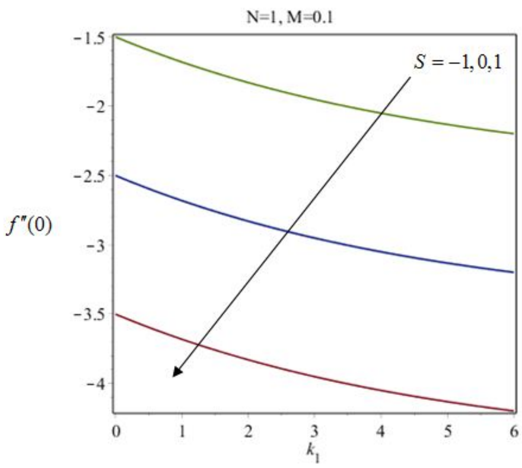

Fig. 11. Skin friction coefficient $f''(0)$ with permeability parameter k_1 for several values of suction/ injection parameter S.

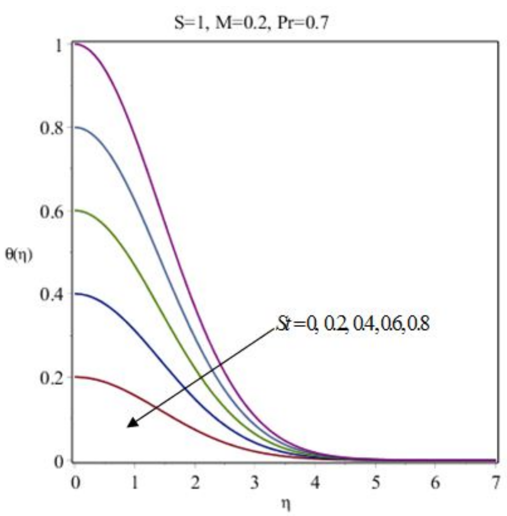

Fig. 12. Variation of temperature $\theta(\eta)$ with η for several values of stratified parameter St in presence of suction.

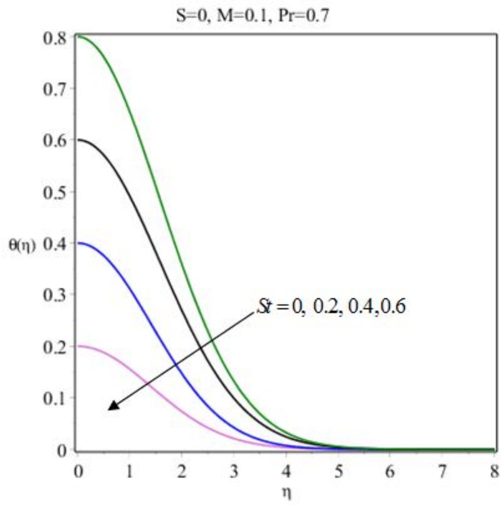

Fig. 13. Variation of temperature $\theta(\eta)$ with η for several values of stratified parameter St in absence of suction $S = 0$.

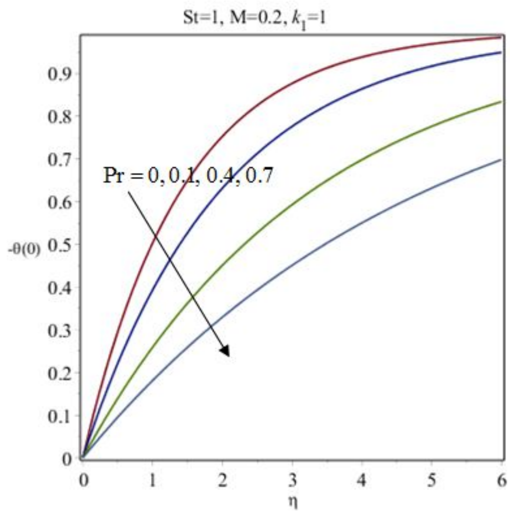

Fig. 14. Variation of heat transfer coefficient $-\theta'(0)$ with η for several values of Prandtl number in absence of suction $S = 0$.

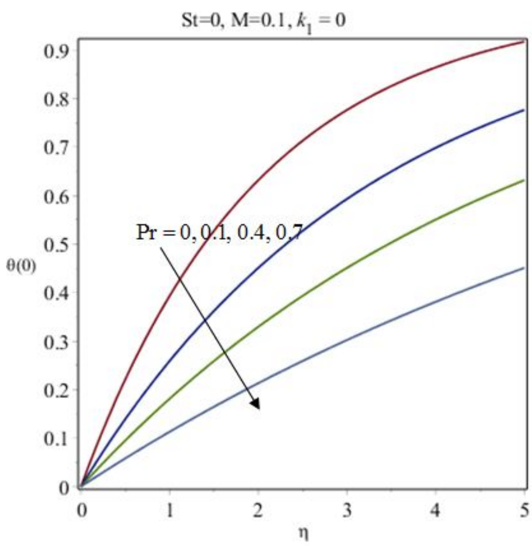

Fig. 15. Variation of heat transfer coefficient $-\theta'(0)$ with η for several values of Prandtl number in presence of suction $S = 1$.

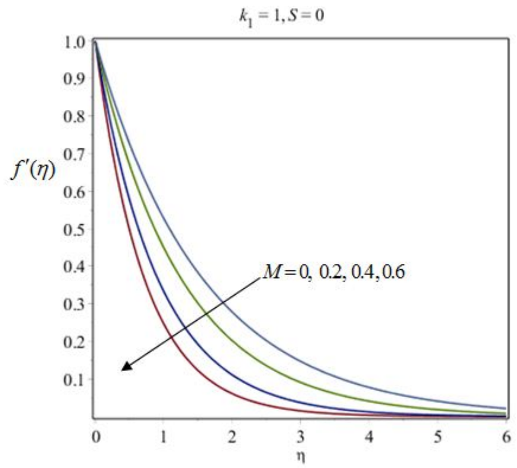

Fig. 16. Variation of velocity $f'(\eta)$ with η for several values of Lorentz force M in absence of suction $S = 0$.

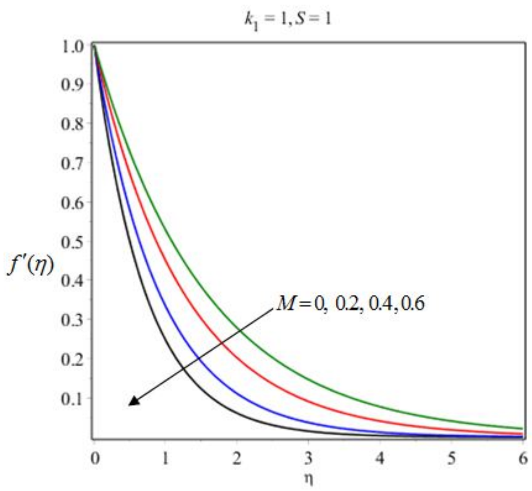

Fig. 17. Variation of velocity $f'(\eta)$ with η for several values of Lorentz force M in presence of suction $S = 1$.

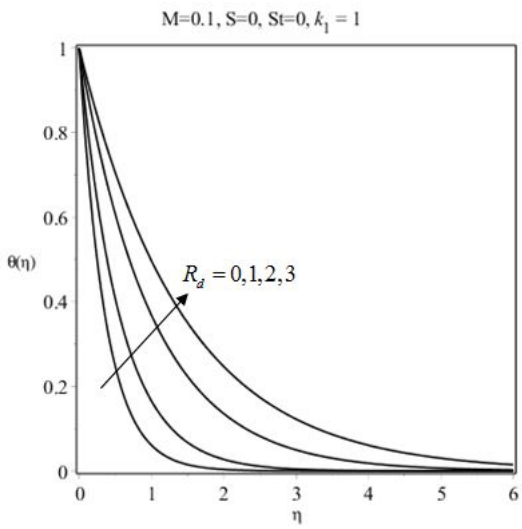

Fig. 18. Variation of temperature $\theta(\eta)$ with η for several values of Radiative parameter R_d in absence of suction $S = 0$.

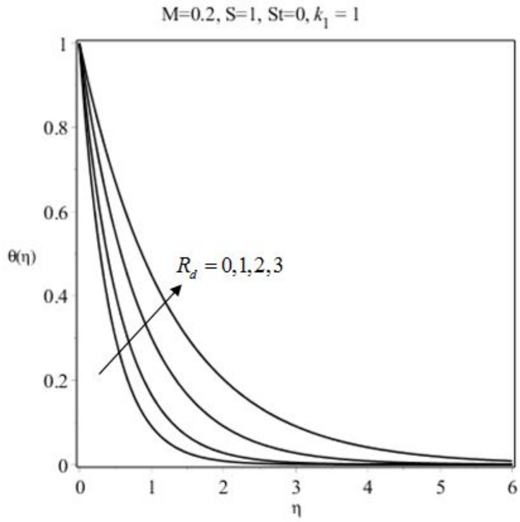

Fig. 19. Variation of temperature $\theta(\eta)$ with η for several values of Radiative parameter R_d in presence of suction $S = 1$.

It is seen that temperature decreases with increases suction whereas it increases due to injection. The effect of suction is to make the velocity and temperature distribution more uniform within the boundary layer. The influence of permeability parameter k_1 in the absence of suction $S = 0$ on velocity profile and presence of suction $S = 1$ are exhibits in Fig. 7 and 8 respectively. It is obvious that the presence of a porous medium causes higher restriction to the fluid flow which, in turn, slows its motion. Therefore the velocity decreases due to porous medium parameter for both suction/injection. While in Fig. 9, the shear stress at the surface increases with increases the permeability parameter k_1 so that the temperature has rise in the boundary layer. Fig. 10, implies that Darcian body force improves the heat transfer rate. It can thus be inferred that an increase in permeability parameter decreases the boundary layer thickness and consequently brings about an increase in the heat transfer rate. Fig. 11 depicts the nature of skin friction coefficient against the permeability parameter k_1. Skin friction coefficient $[-f''(0)]$ increases with increasing permeability parameter. The increase of permeability parameter k_1 leads to increase the skin-friction. The permeability parameter k_1 introduces an additional shear stress on the boundary. Next, we present the effects of thermal stratification parameter St on temperature and temperature gradient profiles in the absence and presence of suction at the boundary. Temperature profile $\theta(\eta)$ for different values of stratified parameter in the presence of suction and absence of suction are presented by Fig. 12 and Fig. 13. It is found that the temperature decreases as the stratified parameter increases. Since the increases of stratification parameter St means increase in free-stream temperature or decrease in surface temperature. Thermal boundary layer thickness is therefore also decreased with increases values of thermal stratification parameter St. In Fig. 14 and Fig. 15, the variation of heat transfer coefficient $-\theta(0)$ on the dimensionless quantity for different values of Prandtl number were plotted. This is shows that the effect of Prandtl number on increasing temperature is decreases. Prandtl number Pr signifies the ratio of momentum diffusivity to thermal diffusivity. In heat transfer problems, the Prandtl number controls the relative thickness of the momentum and thermal boundary layers. When Prandtl number Pr is small, heat diffuses quickly compared to the velocity, which means that for liquids metals, the thickness of the thermal boundary layer is much bigger than the momentum boundary layer. Fluids with lower Prandtl number have higher thermal conductivities so that heat can be diffuse from the sheet faster than for higher Prandtl number fluids. Hence Prandtl number can be used to increase the rate of cooling in conducting flows. Fig. 16 and Fig. 17 represents the effect of magnetic parameter M on the velocity profile with and without suction. The rate of transport decreases with the increases of M as the Lorentz force is increases. It is found that the velocity is decreases with the increasing values of M. Fig. 18 and Fig. 19 depict that the larger values of radiation parameter R_d shows an enhancement in the temperature profile and its related boundary layer thickness. Larger values of radiation parameter provide more heat to working fluid that shows an enhancement in the temperature $\theta(\eta)$ on η for both suction and injection.

5. Conclusions

The series solution of MHD flow and heat transfer of viscous incompressible fluid towards a porous exponential sheet in presence of thermal radiation in stratified medium is investigated. The behavior of embedding parameter is examined. An analytical technique well known as homotopy analysis method (HAM) has been applied to determine the solutions of the governing non-linear ordinary differential Eqs. (24)-(25). Graphical illustrations were shown subsequent to the flow characteristics for the velocity and temperature with the various associated physical parameters. Good agreement of HAM solution is observed with those obtained by numerical methods in Table 1. The effect of suction as well as magnetic parameter on fluid is to suppress the velocity field which turn causes the enhancement of the skin-friction coefficient. Rate of transport is reduced with the magnetic field. The temperature decreases with increases of stratified parameter. All the numerical calculation has been done in `Maple-2015` built-in function `dsolve`.

References

[1] B.C. Sakiadas, Boundary layer behavior on continuous solid flat surfaces, J.A.I.Ch.E.J 7 (1961) 26-28.
[2] F.K. Tsou, E.M. Sparrow, R.J. Goldstein, Flow and heat transfer in the boundary layer on a continuous moving surface, Int.J Heat Mass Transfer 10 (1967) 219-235.
[3] L. Crane, Flow past a stretching plate, ZAMP 21 (1970) 645-647.
[4] C.Y. Wang, Free convection on a vertical stretching surface, J. App Math Mech (ZAMM), 69 (1989) 418-420.
[5] E.M.A. Elbashbeshy, Heat transfer over an exponentially stretching continuous surface with suction, Arch. Mech 53 (2001) 643-651.
[6] S.K. Khan, M.S. Abel, R.M. Sonth, Viscoelastic MHD flow Heat and Mass transfer over a stretching sheet with dissipation of energy and stress work, Heat Mass Trans. 40 (2004) 7-57.
[7] A. Ishak, R. Nazar, I. Pop, Heat transfer over a stretching surface with variable heat flux in micropolar fluids, Phys. Lett. A. 372 (2008) 559-561.
[8] S. Nadeem, S. Zaheer, T. Fang, Effects of thermal radiation on the boundary layer flow of a Jeffrey fluid over an exponentially stretching surface. Numer. Algo. 57 (2011) 187-205.
[9] S. Nadeem, R. Haq, C. Lee, MHD flow of a Casson fluid over an exponentially stretching sheet, Scien. Iran. B 19 (2012) 1550-1553.
[10] P.S. Gupta, A.S. Gupta, Heat and Mass transfer on a stretching sheet with suction and blowing, Can. J. Chem. Eng. 55 (1977) 744-746.
[11] B.K. Dutta, P. Roy, A.S. Gupta, Temperature field in the flow over a stretching sheet with uniform heat flux, Int. Commun. Heat Mass Transf. 12 (1985) 89-94.
[12] C.K. Chen, M.I. Char, Heat transfer of a continuous stretching surface with suction or blowing, J. Math. Anal. Appl. 135 (1988) 568-580.
[13] E. Magyari, B. Keller, Heat and Mass transfer in the boundary layer on an exponentially stretching continuous surface, J. Phys. D: Appl. Phys. 32 (2000) 281-288.
[14] V. Kumaran, G. Ramanaiah, A note on the flow over a stretching sheet, Acta Mech. 116 (1996) 229-233.
[15] H. Xu, S.J. Liao, Series solutions of unsteady Magnetohydrodynamics flows of non-Newtonian fluids caused by an impulsive stretching plate, J. Non-Newtonian Fluid Mech. 159 (2005) 46-55.
[16] R. Cortell, Flow and heat transfer of a fluid through a porous medium over a stretching surface with internal heat generation/ absorption and suction/blowing, Fluid Dyn. Res. 37 (2005) 231-245.
[17] R. Cortell, Effects of viscous dissipation and work done by deformation on the MHD flow and heat transfer of a viscoelastic fluid over a stretching sheet, Phys. Lett. A. 357 (2006) 298-305.
[18] T. Hayat, Z. Abbas, M. Sajid, Series solution for the upper convective Maxwell-fluid over a porous stretching plate, Phys. Lett. A. 358 (2006) 393-403.
[19] T. Hayat, M. Sajid, Analytic solution for axi-symmetric flow and heat transfer of a second grade fluid past a stretching sheet, Int. J. Heat Mass Transf. 50 (2007) 75-84.
[20] I.C. Mandal, S. Mukhopadhyay, Heat transfer analysis for fluid flow over an exponentially stretching porous sheet with surface heat flux in porous medium, Ain Shams Eng. 4 (2013) 103-110.
[21] S. Mukhopadhyay, MHD boundary layer flow and heat transfer over an exponentially stretching sheet embedded in a thermally stratified medium, Alex. Eng. Jour. 52 (2013) 259-265.
[22] B. Bidin, R. Nazar, Numerical solution of the boundary layer flow over an exponentially stretching sheet with thermal radiation, Euro. J. Sci. Res. 33 (2009) 710-717.
[23] M.A. Al-Aziz, Viscous dissipation effect on mixed convection flow of a micropolar fluid over an exponentially stretching sheet, Can. J. Phys. 87 (2009) 359-368.
[24] S.J. Liao, Homotopy analysis method in nonlinear differential equation, Springer, Heidelberg, Germany, 2012.
[25] S.J. Liao, An optimal homotopy analysis approach for

strongly nonlinear differential equations, Commun. Non Lin. Sci. Numer. Simul. 15 (2010) 2003-2016.
[26] S.J. Liao, Advances in the homotopy analysis method, World Scientific, ISBN 978-9814551243, 2013.
[27] F. Mabood, W. Khan, homotopy analysis method for boundary layer flow and heat transfer over a permeable plate in a Darcian porous medium with radiation effects, J. Taiwan Ins. Chem. Eng. 45 (2014) 1217-1224.
[28] M.H. Abolbashari, N. Freidoonimehr, F. Nazari, M.M. Rashidi, Analytical modeling of entropy generation for Casson nano-fluid flow induced by a stretching surface, Adv. Powd. Tech. 2016 Article in Press.
[29] T. Hayat, T. Muhammad, A. Alsaedi, M. S. Alhuthali, Magnetohydrodynamics three dimensional flow of viscoelastic nano-fluid in the presence of nonlinear thermal radiation, J. Magne. Magne. Mat. 385 (2015) 222-229.
[30] T. Hayat, N. Gull, M. Farooq, B. Ahmad., Thermal radiation effect in MHD flow of Powell-Eyring Nanofluid induced by stretching cylinder, J.Aerosp.Eng. ASCE, 2015, DOI: 10.1061.
[31] M. Mustafa, T. Hayat, A. Alsaedi, Unsteady boundary layer flow of nanofluid past an impulsive stretching sheet, J. Mech. 29(3) (2013) 423-432.
[32] M. Turkyilmazoglu, MHD fluid flow and heat transfer due to a shrinking rotating disk, Comput. Fluids, 90 (2014) 51-56.
[33] J. Surawala, M.G. Timol, On the solution of unsteady power law flow near a moving wall by new similarity analysis method, Int. J. Adv. Appl. Math. and Mech. 3(3) (2016) 27-31.
[34] N. Pandya, A.K. Shukla, Effects of radiation and chemical reaction on an unsteady WalterâĂŹs-B viscoelastic MHD flow past a vertical porous plate, Int. J. Adv. Appl. Math. and Mech. 3 (1) (2016) 19-26.
[35] M.F. El-Sayed, H.N.A. Ismail, E. H. Aly, N. F. Aballaha, The stagnation point MHD flow and heat transfer of micropolar fluid over a stretching sheet in presence of radiation, heat generation and dissipations, Int. J. Adv. Appl. Math. and Mech. 3 (2) (2015) 84-99.
[36] T. Raghunath Rao, Peristaltic transport of a Newtonian fluid with wall properties in an asymmetric channel, Int. J. Adv. Appl. Math. and Mech. 3 (1) (2015) 102-109.
[37] G.R. Rajput, J. S.V.R. Krishnanprasad, M. G. Timol, Application of scaling group transformation for MHD boundary layer flow and heat transfer of nanofluids over moving surface subject to suction/ injection in presence of thermal radiation with chemical reaction, Int. J. Adv. Appl. Math. and Mech. 3 (1) (2015) 139-144.
[38] S. Gupta, D. Kumar, J. Singh, Application of HeâĂŹs homotopy perturbation method for solving nonlinear wave-like equations with variable coefficients, Int. J. Adv. Appl. Math. and Mech. 1 (2) (2013) 65-79.
[39] D.D. Joseph, D.A. Nield, G. Papnicolaou, Nonlinear equation governing flow in a saturated porous media, Water Resour. Res. 18 (1982) 1049-1052.
[40] D. Pal, P.S. Hiremath, Computational modeling of heat transfer over an unsteady stretching surface embedded in a porous medium, Meccanica, 45 (2010) 415-424.
[41] H. Brinkman, A calculation of the viscous force exerted by a flowing fluid on a dense swarm of particles, Appl. Sci. Res. A. 1 (1949) 27-34.
[42] K. Vafai, C.L. Tien, Boundary and Inertia effects on flow and heat transfer in porous media, Int. J. Heat Mass Transf. 24 (1981) 195-204.
[43] S. Mukhopadhyay, G.C. Layek, Effects of variable fluid viscosity on flow past a heated stretching sheet embedded in a porous medium in presence of heat source/sink, Meccanica, 58 (2011) 945-953.
[44] F.C. Lai, F.A. Kulacki, The effect of variable viscosity on convective heat and mass transfer along a vertical surface in saturated porous media, Int. J Heat Mass Transf. 33 (1991) 1028-1101.
[45] S.J. Liao, Notes on the homotopy analysis method: some definitions and theorems, Commun. Nonlinear Sci. Numer. Simul. 14 (2009) 983-991.